AD-A145 091 A DETERMINATION OF THE PHOTOCHEMICAL QUANTUM YIELDS 1/1
FROM TWO EXCITED TRIP..(U) IBM RESEARCH LAB SAN JOSE CA
R K GRYGIER ET AL. 10 AUG 84 TR-7 N00014-81-C-0418
UNCLASSIFIED F/G 7/5 NL

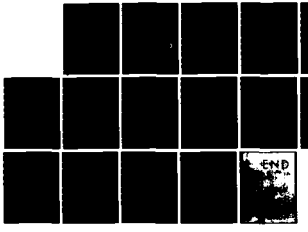

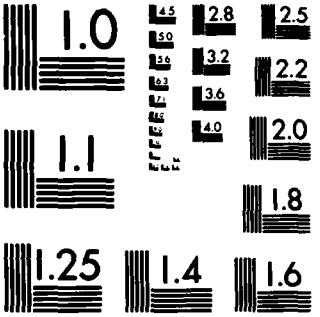

965 · IBM · 05

(12)

Unclassified
SECURITY CLASSIFICATION OF THIS PAGE (When Data Entered)

REPORT DOCUMENTATION PAGE		READ INSTRUCTIONS BEFORE COMPLETING FORM
1. REPORT NUMBER: 7	2. GOVT ACCESSION NO.	3. RECIPIENT'S CATALOG NUMBER
4. TITLE (and Subtitle): A Determination of the Photochemical Quantum Yields from Two Excited Triplet States of Biacetyl Using Holography		5. TYPE OF REPORT & PERIOD COVERED: Technical Report 6. PERFORMING ORG. REPORT NUMBER
7. AUTHOR(s): R. K. Grygier, P.-A. Brugger, D. M. Burland		8. CONTRACT OR GRANT NUMBER(s): N00014-81-C-0418
9. PERFORMING ORGANIZATION NAME AND ADDRESS: International Business Machines Corp. San Jose Research Laboratory 5600 Cottle Road, San Jose, CA 95193		10. PROGRAM ELEMENT, PROJECT, TASK AREA & WORK UNIT NUMBERS
11. CONTROLLING OFFICE NAME AND ADDRESS: Office of Naval Research Code 413 800 N. Quincy Street Arlington, VA 22217		12. REPORT DATE: August 10, 1984 13. NUMBER OF PAGES: 28
14. MONITORING AGENCY NAME & ADDRESS(if different from Controlling Office)		15. SECURITY CLASS. (of this report): Unclassified 15a. DECLASSIFICATION/DOWNGRADING SCHEDULE

16. DISTRIBUTION STATEMENT (of this Report)

This document has been approved for public release and sale; its distribution is unlimited.

17. DISTRIBUTION STATEMENT (of the abstract entered in Block 20, if different from Report)

DTIC ELECTE AUG 2 2 1984 S B

18. SUPPLEMENTARY NOTES

To be published in Journal of Physical Chemistry

19. KEY WORDS (Continue on reverse side if necessary and identify by block number)

Photochemistry, Quantum Yields, Holography

20. ABSTRACT (Continue on reverse side if necessary and identify by block number)

A holographic technique has been used to measure the quantum yield for photochemical product formation from two excited triplet states of biacetyl in a polymer host. The technique involves a simple measurement of the time taken for the hologram to reach its maximum diffraction efficiency. This measured time can be directly related to a photochemical quantum yield. The diffraction efficiency from the lowest triplet state has a yield of 0.045±0.010 measured in this way as compared to a value of 0.03±0.005 determined using a direct absorption method. The triplet state 13,000 cm^{-1} above the lowest triplet state

AD-A145 091

DTIC FILE COPY

965 · IBM · 05

DD FORM 1 JAN 73 1473 84 08 22 014

Unclassified
SECURITY CLASSIFICATION OF THIS PAGE (When Data Entered)

OFFICE OF NAVAL RESEARCH

Contract N00014-81-C-0418

Task No. NR 051-782

TECHNICAL REPORT NO. 7

A Determination of the Photochemical Quantum Yields From Two Excited Triplet States of Biacetyl Using Holography

by

R. K. Grygier
P.-A. Brugger
D. M. Burland

Prepared for Publication

in

Journal of Physical Chemistry

IBM Research Laboratory
San Jose, California 95193

August 10, 1984

I. INTRODUCTION

A holographic technique has been developed recently for the investigation of photochemical reactions in the solid state [2]. The technique is particularly useful for investigating photochemical reactions that occur in two steps and require two photons, *i.e.*, photochemical production of a metastable state such as the lowest triplet followed by subsequent excitation to a more highly excited state from which photochemistry occurs [3]. The technique is a zero-background technique and by comparison to direct absorption spectroscopy is much more sensitive to small photochemical changes [4].

In this paper the use of the holographic technique for direct determination of the quantum yield of a photochemical reaction will be described. Examples of its use for both one and two step processes will be given. In treating the two step process, it will be shown that the holographic technique can be used to obtain photochemical quantum yields for reactions that occur as a consequence of triplet-triplet absorption. The experimental reaction used to illustrate both one and two step processes involves the excitation and reaction of biacetyl in a polymer host matrix. Biacetyl undergoes a hydrogen abstraction upon one step excitation of its lowest triplet state [5]. The exact nature of its reaction from the higher triplet state excited in the two step process is not known in detail although it has been shown to differ from the lowest triplet reaction and to be consistent with an α-cleavage mechanism [6].

Recently, Deeg *et al.* [7] have developed a holographic technique complementary to the one described here, that permits one to obtain photochemical quantum yields when the index of refraction difference between reactants and products is known. By comparison the technique described in this paper requires a knowledge of the extinction

coefficient at the hologram recording wavelength and, for a two step process, the lifetime of the metastable state.

In the next section the relationship between the kinetic rate equations for one and two step processes and hologram growth is described. Simple expressions for the relationship between hologram growth parameters and photochemical quantum yields are presented. In Section III the details of the hologram experiment are described as is the preparation of biacetyl/polymer samples. In Section IV the use of the holographic technique to obtain quantum yields for both one and two step processes is demonstrated from experimental measurements on biacetyl. Knowing the quantum yields from Section IV, one can check the validity of the theoretical framework by calculating other features of hologram growth and comparing these calculated quantities with experiment. This is done in Section V. As a result of this analysis, it is shown that one can obtain the index of refraction change between reactants and photochemical products at the hologram recording wavelength.

II. RELATIONSHIP BETWEEN HOLOGRAPHY AND PHOTOCHEMISTRY

A. General Features of Holography

A generalized diagram of the production of a hologram is shown in Figure 1. Two coherent beams are superimposed on the holographic sample. For the present they will be considered to be plane waves, a reference wave with intensity I_R and an object wave with intensity I_0. The object wave is not completely absorbed by the sample. The major part of the beam passes through the sample.

At the point where object and reference beam overlap, an interference pattern is produced. The plane wave interference pattern is a simple cosine modulation of the intensity across the sample:

$$I(x) = (I_R + I_0)\left[1 + V \cos\left(\frac{2\pi x}{\Lambda}\right)\right] \tag{1}$$

where V is the fringe contrast and is given by

$$V = 2\sqrt{I_R I_0}/(I_R + I_0) \tag{2}$$

and the fringe spacing Λ is given by

$$\Lambda = \frac{\lambda}{(2\bar{n}\sin\theta)} . \tag{3}$$

In Eq. (3), λ is the recording wavelength, θ is the angle of incidence shown in Figure 1 and $\bar{n}$ is the average index of refraction of the holographic medium.

The spatially nonuniform intensity pattern described in Eq. (1) results in a nonuniform distribution of photoproducts across the sample. A consequence of this spatial inhomogeneity in the chemical composition and optical properties of the sample is the diffraction of a portion of the reference beam into the direction of the original object beam, whether or not the object beam is present.

If the intensity of the light diffracted by the hologram is I, one can define a hologram efficiency η as

$$\eta = \frac{I}{I_R} . \tag{4}$$

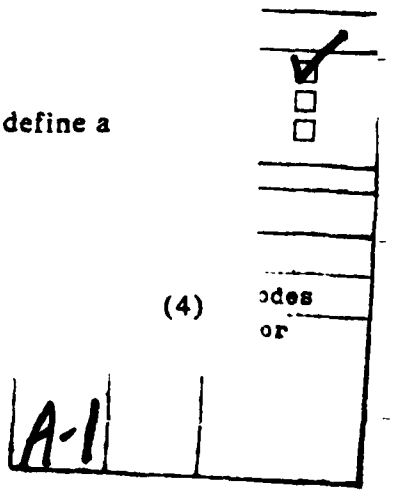

Kogelnick [8] has shown that in the absence of absorption effects (which are negligible in the cases treated here) and when the sample thickness d is much larger than the fringe spacing this efficiency is given by

$$\eta = \sin^2\left(\frac{\pi n_1 d}{\lambda \cos\theta}\right). \tag{5}$$

It is assumed in Eq. (5) that the nonuniform index of refraction across the sample which is a direct consequence of the nonuniform photochemistry may be written

$$n = n_0 + n_1 \cos\left(\frac{2\pi}{\Lambda} x\right) + n_2 \cos\left(\frac{4\pi}{\Lambda} x\right) + \ldots . \tag{6}$$

All of the photochemical information that can be obtained from a holographic experiment is contained in n_1. This can be seen if we consider a photochemical reaction that begins with a reactant A with molar concentration [A] and results in a product P with molar concentration [P]. The index of refraction of the medium (ignoring any background contribution from the host) is then given by

$$n = \delta n_A[A] + \delta n_P[P] \tag{7}$$

where δn_A and δn_P are the index of refraction increments produced by a one molar concentration of A or P. Having expressions for [A] and [P] as a function of time and space one can then use Eq. (5) to calculate the temporal behavior of the hologram.

B. One Step Photochemical Processes

The energy level scheme for a one step photochemical process is shown in Figure 2a. The ground state of a molecule A is excited by light to a metastable excited state B which can either react to form products P or return to the ground state. For the biacetyl molecule of interest in this paper, the actual energy level scheme is

somewhat more complicated than is shown in Figure 2. Biacetyl absorption occurs from the ground state to the lowest singlet state. Photochemistry occurs after intersystem crossing to the lowest triplet. Since the quantum yield for intersystem crossing is very close to 1.0 [9], it is perfectly reasonable to treat biacetyl according to the scheme in Figure 2a. The rate constant k_1, then describes absorption to the lowest singlet and k_2 radiative and radiationless relaxation of the lowest triplet state.

The lowest singlet state of biacetyl is excited using the 457.9 nm line of an Ar^+ laser. The rate constant at a point x in the medium is thus given by [2]

$$k_1(x) = 2303.\epsilon_1 I(x) \tag{8}$$

$$\equiv k_1^0\left[1 + V\cos\frac{2\pi}{\Lambda}x\right]$$

where ϵ_1 is the molar extinction coefficient and where I(x) is given by Eq. (1) and has units of einsteins/cm^2sec. The constant k_1^0 is equal to $2303.\epsilon_1 I_0$, where I_0 is the intensity of one of the interfering beams.

In the limit where $k_2+k_3 \gg k_1$, which is always the case for a low enough light intensity, the kinetic rate equations describing the process outlined in Figure 2a can be solved in the steady state approximation to yield:

$$[A] = A_0\, e^{-\Phi k_1 t} \tag{9}$$

$$[P] = A_0 - [A] \tag{10}$$

where A_0 is the initial concentration of A and where

$$\Phi \equiv \frac{k_3}{k_2 + k_3} \tag{11}$$

is the quantum yield of photochemistry, the quantity that one ultimately hopes to determine.

Using Eqs. (7), (9) and (10), an expression may be derived for that portion of the total index of refraction that has spatial variation:

$$n(x) = (\delta n_A - \delta n_P) A_0 \exp(-\Phi k_1(x) t) . \tag{12}$$

Replacing $k_1(x)$ in Eq. (12) and expanding the resulting exponential in a Fourier cosine series, one obtains for n_1, defined by Eq. (6), the expression [10]:

$$n_1 = 2(\delta n_P - \delta n_A) A_0 \exp(-k_1^0 \Phi t) I_1(V k_1^0 \Phi t) . \tag{13}$$

where $I_1(z)$ is a modified Bessel function of order 1.

According to Eq. (5), the efficiency η can have a maximum value for two reasons. First the argument of the sin can become an odd multiple of $\pi/2$ at which point the efficiency reaches a maximum value of unity [11]. For all of the situations treated in this paper the maximum efficiencies are less than unity and this case is not of importance.

The efficiency may also reach a maximum value because n_1 itself has a maximum. This occurs when the following equality is satisfied

$$I_1(V k_1^0 \Phi t_m)\left(\frac{1}{V} + \frac{1}{k_1^0 \Phi t_m}\right) = I_0(V k_1^0 \Phi t_m) \tag{14}$$

where t_m is the time taken for the hologram to reach its maximum efficiency. Solving this transcendental equation for t_m yields

$$\frac{1}{t_m} = \frac{k_1^0 \Phi V}{f(V)} \tag{15}$$

where f(V) is a slowly varying function of V for beam intensity ratios (I_r/I_0) between 0.8 and 1.2 For V equal to unity $f(1.0)$ is 1.545. This value is used in all subsequent discussions.

Equation (15) suggests a simple way of determining the quantum yield for a solid state photochemical reaction by making a measurement of the time required for a hologram to reach its maximum efficiency. The only additional experimental quantities one needs to know are the exciting light intensity and the absorption coefficient.

The derivation in this section has assumed two interfering plane wave beams. In many experimental cases including the ones described here the two beams are better described as Gaussian. In this case the appropriate intensity to use for I_0 is the peak intensity. The value of t_m is also changed by about 20% from the value that would be obtained for the same parameters but recording with plane waves. The appropriate equations for arbitrarily shaped beams are derived in the Appendix. All experimental quantum efficiencies reported in this paper have assumed a Gaussian profile for the interfering laser beams.

C. Two Step Photochemical Processes

The energy level scheme for a two step process is shown in Figure 2b. In this process the ground state of the system is excited to an intermediate level B at an intensity dependent rate k_1. The state B, which may be a composite state as in the one step process, relaxes back to the ground state at a rate k_2. The state B may itself be excited to the state C by light of the same or a different wavelength. State C may either relax back to B or react to form products.

It is straightforward to show, utilizing a steady state approximation for the concentration of B, that the kinetic scheme in Figure 2b can be replaced by the one shown in Figure 2c where now

$$\Phi = \frac{k_5}{k_4 + k_5} . \tag{16}$$

The two step process now sufficiently resembles the one step kinetic scheme of Figure 2a that one can immediately write the solutions:

$$[A] = A_0 \exp\left[\frac{-k_1 k_3 \Phi}{k_1 + k_2} t \right] \tag{17}$$

$$[P] = A_0 - [A] . \tag{18}$$

There are differences however. Both k_1 and k_3 depend on an exciting light intensity for the two step process. The hologram is produced, as will be discussed in the next section, by the transition described by k_3. k_3 thus has a spatial dependence similar to that described by Eq. (8). For the experiments on biacetyl the A→B transition was excited by 457.9 nm light so that

$$k_1 = 2303. \epsilon_1 I_1 \tag{19}$$

where I_1 is constant across the sample. The B→C transition utilized two interfering beams at 752.5 nm and

$$k_3 = 2303. \epsilon_1 I_2(x) . \tag{20}$$

Here $I_2(x)$ is defined as for the one step process by Eq. (1). Utilizing exactly the same procedure that resulted in Eq. (15), one obtains the following expression for the two step process

$$\frac{1}{t_m} = \frac{k_1 k_3^0 \Phi}{1.545 k_2} \tag{21}$$

in the case where V=1. The quantum yield for a two step process can be obtained assuming one knows the intensities I_1 and I_2, the molar extinction coefficients ϵ_1 and ϵ_2 at the two different wavelengths and the lifetime $\tau=1/k_2$ of state B.

III. EXPERIMENTAL DETAILS

A. Apparatus

The set up for the one step holographic photochemistry experiments is shown in Figure 3a. The light from an Ar^+ laser operating at 457.9 nm is split into two beams of equal intensity. These two beams are directed through a 2 mm circular aperture onto the holographic sample. The angle corresponding to θ in Figure 1 is 2.8°. The corresponding fringe spacing Λ is thus 4.7 μm.

The growing hologram is continuously monitored at the Bragg angle by a HeNe laser beam chopped at 200 Hz that also passes through the aperture. The portion of the incident HeNe laser light that is diffracted by the hologram passes through an aperture and an interference filter and strikes a photodiode/amplifier combination detector. The electrical signal at 200 Hz from this detector is amplified by a lock-in amplifier and sent to an IBM Series/1 computer for data collection and analysis. The laser and all optical components are mounted on a floating vibration isolation table and the optical components are enclosed in a box to reduce the effects of air currents.

In those cases where absolute hologram efficiencies η or hologram growth rates ($d\sqrt{\eta}/dt$) must be determined, the efficiency measured at 632.8 nm is converted to the wavelength used to create the hologram using a linear conversion factor. This factor is

obtained by comparing the efficiencies of the hologram measured at the two wavelengths.

For the 1.0 M biacetyl in polymeric matrix samples used, the average biacetyl-biacetyl intermolecular distance is only a few nanometers. At these close distances it is quite possible that intramolecular energy transfer can affect the kinetic results. It was shown, however, that, with biacetyl concentrations ranging from 0.2 to 1.5M, the holographic properties η, $d\sqrt{\eta}/dt$ and t_{max} followed the expected dependances with amount of light absorbed in the various samples. This shows that biacetyl-biacetyl intermolecular energy transfer can be excluded as a major pathway in our kinetic scheme.

Since the biacetyl/polymer samples were prepared by slow evaporation of toluene, we have also checked the effect of residual toluene in the polymer. No difference in any of the measured holographic parameters was observed when quantitatively dried 1.0 M biacetyl in polystyrene is compared with a sample containing up to 5% by weight of residual solvent. And finally, the holographic properties are independent over a wide range of host polymer molecular weights.

The two step experimental set up is similar to the one step one and is shown in Figure 3b. In this case the two interfering beams that produce the hologram are produced by a Kr^+ laser operating at 752.5 nm. The angle of incidence θ is 4.2°, giving a fringe spacing Λ of 4.7 μm as for the one photon case. To increase the power density incident on the hologram sample, the two beams are focused to a spot size of about 100 μm (FWHM). Care is taken to insure that both beams have the same size

and intensity and overlap at the sample so that the fringe contrast V is very nearly unity.

The first step in this two step process is pumped by an Ar^+ laser operating at 457.9 nm. This beam is considerably larger than the two infrared beams. As before all optics are on a vibration isolation table inside of a box. The hologram detection scheme is the same as for the one step process.

Quantum yields for the one step photochemical process are determined by following the disappearance of the biacetyl absorption as the sample is illuminated at 457.9 nm. The lifetime of biacetyl samples is determined by averaging 256 shots from a 5 Hz nitrogen pumped pulsed dye laser at 443 nm. The decay of the phosphorescence emission was detected at 520 nm.

B. Sample Preparation

For the one step process samples are made by dissolving 1.0 M dried and distilled biacetyl (Aldrich) in an unpolymerized cyanoacrylate monomer. The solution is squeezed between two microscope slides with 200 μm cover glass spacers. The cyanoacrylate is allowed to polymerize for 24 hours before use in the experiments.

For the two step process 1.0 M biacetyl in polystyrene is used. The high purity polystyrene (Polysciences, Inc., Cat. No. 16231) has an average molecular weight of 10,200 according to the manufacturer. The samples are prepared by first dissolving the biacetyl and polystyrene together in toluene. The solution is dropped onto a microscope slide and the toluene allowed to evaporate slowly. This step is done in saturated biacetyl atmosphere to inhibit the evaporation of biacetyl from the thin sample. The samples sit overnight in the biacetyl atmosphere. They are then gently

heated to soften the polymer and squeezed between two glass microscope slides to a thickness of about 250 μm.

IV. QUANTUM YIELD MEASUREMENTS

The biacetyl molecule is particularly appropriate for illustrating the use of the holographic technique for measuring quantum yields. As Figure 4 illustrates, biacetyl undergoes both one and two step photochemical processes. The one step process occurs from T_1 and the two step process from T_n.

The one step process corresponds to the situation described in Section IIB and, according to Eq. (15), the quantum yield can be obtained from a measurement of t_m. Typical hologram growth curves are shown in Figure 5. From the figure one can see that, as the exciting light intensity is reduced, the time for the hologram to reach its maximum efficiency increases. According to Eqs. (8) and (15) a plot of $1/t_m$ *versus* exciting light intensity should yield a straight line from whose slope the quantum yield can be obtained, provided one knows the singlet-singlet molar extinction coefficient at the exciting wavelength. Such a plot is shown in Figure 6. As mentioned previously, care must be taken in measuring the laser light intensity to account for the spatial profile of the laser beam (see the Appendix).

From a least squares fit of the straight line and measurement of ϵ_1 at 457.9 nm (ϵ_1=8.5ℓ/mole cm) the quantum yield of photoproduct formation is determined to be 0.045 ± 0.01. This should be compared to a value of 0.03 ± 0.005 measured directly by following the disappearance upon irradiation of the biacetyl absorption spectrum. Within the experimental error, the agreement here between the holographic technique and the direct absorption method illustrates the general validity of the technique. To

achieve improved accuracy several parameters need to be more carefully measured. In particular it is important to know the exact profile of the laser beam.

The two step photochemical process is described by Eq. (21). In addition to knowing ϵ_1, one must know $k_2=1/\tau$ and ϵ_2 in order to determine the quantum yield. ϵ_1 can be determined as before by direct absorption measurements on biacetyl in polystyrene. For this host $\epsilon_1=10.0\ell$/mole cm at 457.9 nm. The triplet lifetime is very sensitive to the host material and sample lifetime. For the system studied here it has been measured to be 55 μsec.

Equation (21) suggests that a plot of $1/t_m$ should yield a straight line when plotted against the light intensity at ω_1 (457.9 nm) or ω_2 (752.5 nm). Figure 7 shows that this is in fact the case for low enough power densities. Above 1.2 kW/cm^2 the increase in t_{max} results from a partial erasing of the diffraction grating at long recording time, due to softening by heating of the polymer matrix. From the slopes of the two straight lines and using Eq. (21) the product $\epsilon_2\phi$ can be determined to be 326ℓ/mole cm. This value for $\epsilon_2\phi$ has actually been determined from least squares fits of $1/t_{max}$ *versus* 457.9 nm power density for several values of the infrared power density and conversely from $1/t_{max}$ *versus* infrared intensity for several 457.9 nm power densities.

The value of ϵ_2 for the triplet-triplet absorption of biacetyl in polystyrene at 752.5 nm is not known. An estimate has been obtained by determining the area under the gas phase triplet-triplet absorption spectrum for biacetyl obtained by Hunzicker [12]. If the oscillator strength for this electronic state is assumed to be constant irrespective of environment, one can use the gas phase spectrum to calibrate the spectra

obtained by Singh *et al.* [13] in carbon tetrachloride, isopropyl alcohol and benzene. ϵ_2 at 752.5 nm obtained from the solution values calibrated in this way is 477ℓ/mole cm. This leads to a value of 0.68 ± 0.02 for ϕ.

V. CALCULATION OF HOLOGRAM GROWTH RATES AND REFRACTIVE INDICES

In this section the numerical values obtained in the previous section will be used to fit experimental data for the hologram growth rate. The growth rate is defined as $d\sqrt{\eta}/dt$ and for very early times in the hologram growth process is given from Eq. (5) by

$$\frac{d\sqrt{\eta}}{dt} \approx \frac{\pi d}{\lambda \cos} \frac{dn_1}{dt} . \tag{22}$$

For a one step process n_1 is given by Eq. (13). For the two step process n_1 is given by Eq. (13) with the substitution of

$$\frac{k_1 k_3^0 \Phi}{k_1 + k_2} \quad \text{for} \quad \Phi k_1^0 .$$

All of the parameters necessary for calculating the hologram growth rate from Eq. (22) are known except the difference in molar index of refraction between the unreacted biacetyl molecule and the products.

Figure 8 shows experimental values of $d\sqrt{\eta}/dt$ *versus* both infrared (752.5 nm) and blue (457.9 nm) light intensity. The detrimental effect of power densities above 1.2 kW/cm^2 seen in Figure 7b are not observed here since the growth rate measurements shown in Figure 8 were evaluated at early stages of the hologram recording. The straight line in both curves is fit to a value of

$$|\delta n_A - \delta n_p| = 5.4 \times 10^{-4} .$$

Figure 8 illustrates two points: first that the kinetic scheme of Figure 2c correctly describes the biacetyl two step process and that the equations derived using this scheme are appropriate for biacetyl, and second that it is possible from these measurements to extract, in addition to the quantum yield, values for the difference in index of refraction between unreacted molecules and photoproducts.

IV. CONCLUSION

In this paper it has been demonstrated that one can obtain values for photochemical quantum yields in both one and two step processes by a simple measurement of the time that it takes for a hologram to reach its maximum efficiency. As an example the reaction of biacetyl in a polymer host has been used. This molecule reacts from its lowest triplet state and from a higher triplet state. The holographic technique has been used to show that the lowest triplet state reaction has a quantum yield of 0.045 ± 0.01 and the upper triplet state reaction a yield near unity.

ACKNOWLEDGMENTS

The authors are grateful to the Office of Naval Research and the U.S. Army Research Office for partial financial support.

APPENDIX

In many cases the assumption of interfering plane waves, that lead to Eq. (5) is not correct. Particularly when the light source is a laser, a Gaussian spatial profile would be more appropriate. The Gaussian nature of the holographic beams can limit the maximum efficiency that a hologram can achieve [14] and it can affect measurements based on knowing the hologram growth rates [7]. In this appendix the effect of the beam profile on the value obtained for t_{max} is discussed.

Assume that one can define a local hologram efficiency η_ℓ valid at a point r in the medium by

$$\eta_\ell = \sin^2\left(\frac{\pi d}{\lambda\cos\theta}\, n_1(r)\right). \tag{A-1}$$

The local value of n_1, here called $n_1(r)$ is given, by analogy with Eq. (13), as

$$n_1(x) = 2(\delta n_P - \delta n_A)A_0 \exp[-k_1^0(r)\Phi t] I_1[k_1^0(r)\Phi t] \tag{A-2}$$

$k_1^0(r)$ in Eq. (A-2) is defined from Eq. (8) as

$$k_1^0(r) = 2303.\epsilon_1 I_0(r) \tag{A-3}$$

for the one photon case or more generally

$$k_1^0(r) = CI_0(r) \tag{A-4}$$

where C is a constant for a given material and $I_0(r)$ expresses the fact that the overlapping incident beams have a spatial intensity variation.

Given these equations, η_ℓ can be written

$$\eta_\ell = \sin^2\{F \exp[-GtS(r)] I_1[GtS(r)]\} \tag{A-5}$$

where

$$F = \frac{\pi d}{\lambda \cos\theta}\, 2(\delta n_P - \delta n_A)A_0$$

$$G = CI_0$$

and where the intensity variation has been written

$$I_0(r) = I_0 S(r) \,. \tag{A-6}$$

To calculate a total diffraction intensity assuming a reconstruction beam profile also given by Eq. (A-6), one can write the locally diffracted intensity $I_\ell(r)$ as

$$I_\ell(r) = I_0(r)\eta_\ell(r) \,. \tag{A-7}$$

The total diffracted intensity is then given by

$$I_{total} = \int_0^\infty I_\ell(r) 2\pi r dr \tag{A-8}$$

and a total diffraction efficiency by

$$\eta_{total} = \frac{I_{total}}{2\pi I_0 \int_0^\infty S(r) dr} \,. \tag{A-9}$$

Equation (A-9) is not universally valid. Writing and reconstruction beams have all been assumed to have an identical form, given by Eq. (A-6). Furthermore, in writing Eq. (A-2), it has been implicitly assumed that the intensity variation described by Eq. (A-6) is small over regions on the order of the fringe spacing. Both of these assumptions are valid for the experiments discussed in this paper. In cases where they are not valid, a more detailed treatment is appropriate [15].

As examples of the application of Eq. (A-9), two cases will be considered. First consider the case where the reacting material responsible for the hologram is far from being depleted. In this case

$$Gt \ll 1$$

and Eq. (A-5) may be written

$$\eta_\ell \cong \sin^2[FGtS(r)/2] . \tag{A-10}$$

In the plane wave case

$$\begin{aligned} S(r) &= 1 \qquad r<d \\ &= 0 \qquad \text{otherwise} \end{aligned} \tag{A-11}$$

where d is the beam halfwidth. Using Eqs. (A-6)-(A-10), one obtains for the total hologram efficiency in the plane wave case

$$\eta_{total} = \sin^2[FGt/2] . \tag{A-12}$$

For Gaussian writing and reading beams

$$S(r) = e^{-r^2/b^2} . \tag{A-13}$$

This case yields

$$\eta_{total} = \left[1 - \frac{\sin(FGt)}{FGt}\right] \tag{A-14}$$

For the limit of no depletion of the reacting material, it can be seen that the plane wave hologram achieves a maximum efficiency of 100% but the Gaussian beam hologram reaches a maximum of only 61%. This limit has been previously discussed [14].

The second case to consider is the general case where the photochemically active material may be used up. For the plane wave the integrations of Eq. (A-8) and (A-9) yield

$$\eta_{total} = \sin^2[F\exp(-Gt)I_1(Gt)] \qquad \text{(A-15)}$$

which reaches a maximum in a time given by Eq. (14). The corresponding integral for the general Gaussian case must be evaluated numerically.

To compare the values of t_{max} obtained for plane and Gaussian beams, it was assumed that the two beams had equal total power and that the Gaussian width is half of the plane wave width. This is equivalent to assuming that the peak Gaussian intensity was twice the average plane wave intensity. In this case the ratios of the time to reach maximum efficiency for the two beams was found to be

$$\frac{t_{max}^{plane}}{t_{max}^{Gauss}} = 0.82$$

irrespective of the intensity of the writing beams (provided of course that the power densities were equal). This factor can be used to correct for the Gaussian nature of the interfering beams. For more complex beam profiles the correction factor will be different of course. The factor can, however, be obtained knowing the beam shape by numerical integrations Eq. (A-9).

REFERENCES

1. IBM Postdoctoral Fellow. Current Address: Institut de Chimie Physique, Ecole Polytechnique Federale, CH-1015 Lausanne, Switzerland.
2. D. M. Burland, G. C. Bjorklund and D. C. Alvarez, *J. Am. Chem. Soc.* **102**, 7117 (1980); G. C. Bjorklund, D. M. Burland and D. C. Alvarez, *J. Chem. Phys.* **73**, 4321 (1980).
3. Chr. Bräuchle, D. M. Burland and G. C. Bjorklund, *J. Am. Chem. Soc.* **103**, 2515 (1981); U. Schmitt and D. M. Burland, *J. Phys. Chem.* **87**, 720 (1983).
4. D. M. Burland, *Accts. Chem. Res.* **16**, 218 (1983).
5. B. M. Monroe, *Adv. Photochem.* **8**, 77 (1971).
6. U. Schmitt and P.-A. Brugger, unpublished results.
7. F. W. Deeg, J. Pinsl, Chr. Bräuchle and J. Voitlander, *J. Chem. Phys.* **79**, 1229 (1983).
8. H. Kogelnik, *Bell System Tech. J.* **48**, 2909 (1969).
9. H. H. Richtol and F. H. Klappmeier, *J. Chem. Phys.* **44**, 1519 (1966); A. A. Lamola and G. S. Hammond, *J. Chem. Phys.* **43**, 2129 (1965).
10. M. Abramowitz and I. A. Stegun, Eds., Handbook of Mathematical Functions (U.S. Gov. Printing Office, Washington, DC, 1972), p. 376.
11. J. C. Urbach and R. W. Meier, *Appl. Opt.* **8**, 2269 (1969).
12. H. Hunzicker, unpublished results.
13. A. Singh, A. R. Scott and F. Sopchyshyn, *J. Phys. Chem.* **73**, 2633 (1969).
14. V. Gerbig, R. K. Grygier, D. M. Burland and G. Sincerbox, *Opt. Lett.* **8**, 404 (1983).
15. R. Guther and S. Kusch, *Sov. J. Quant. Electron.* **6**, 509 (1976).

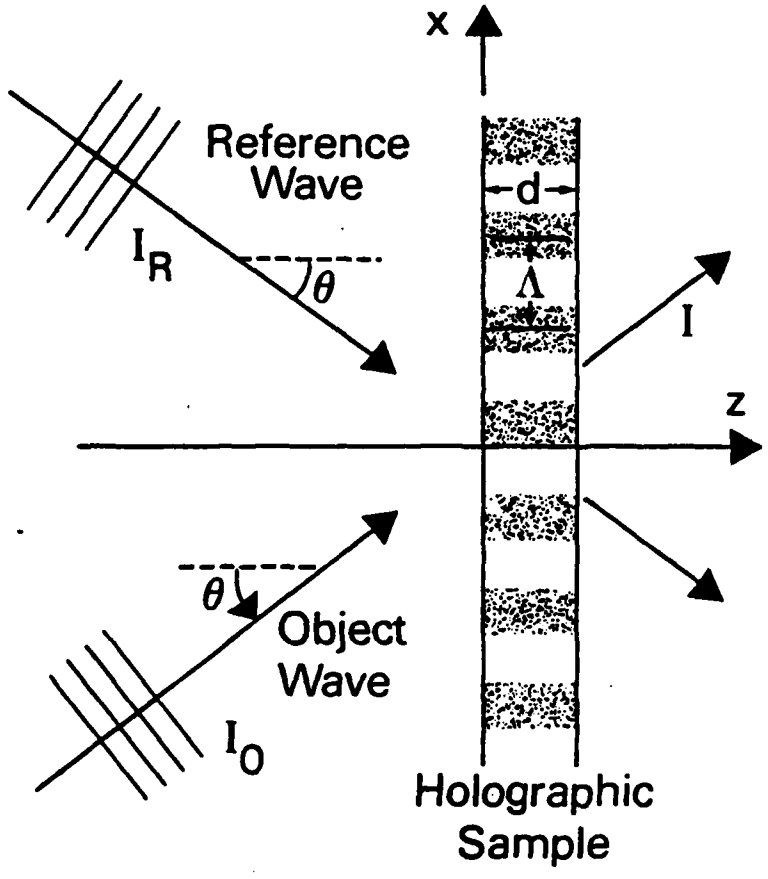

Figure 1. Formation of a hologram by the interference of plane object and reference waves.

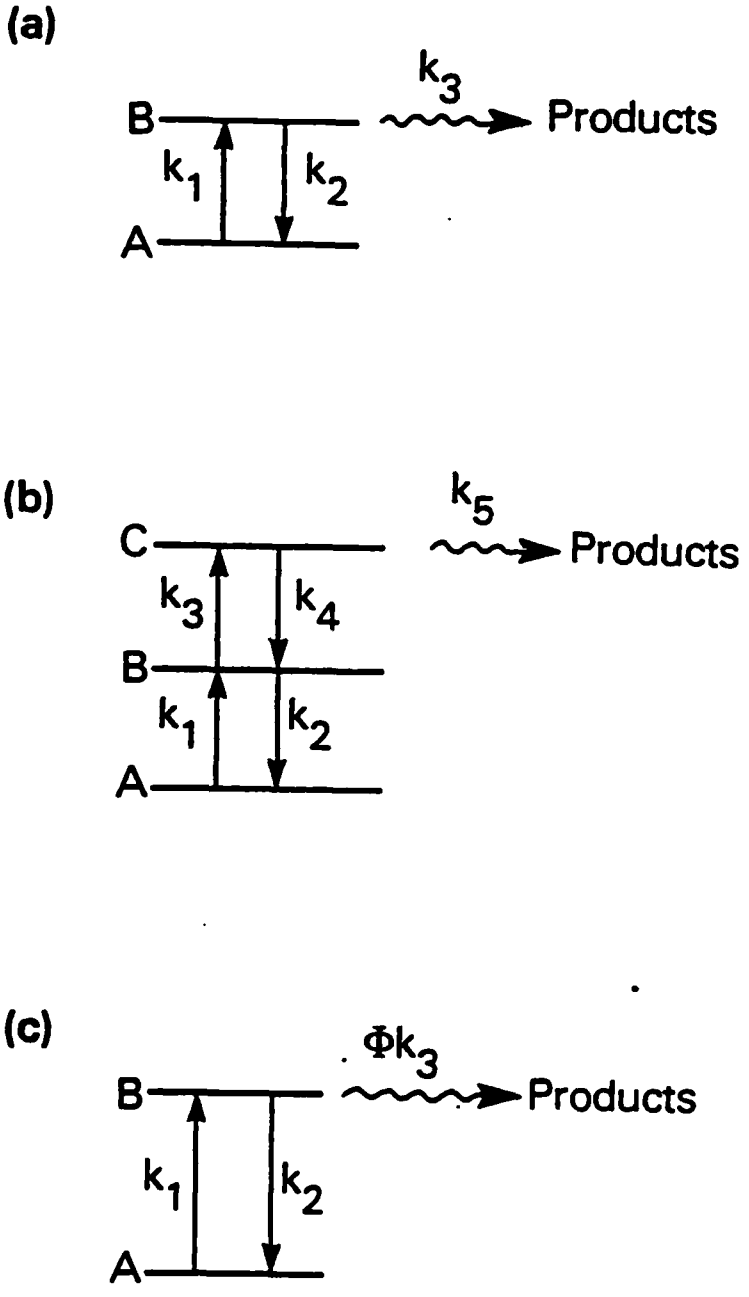

Figure 2. Kinetic schemes for photochemical production of products for a) a one step process and b) a two step process. c) is the reduced kinetic scheme for the two step process assuming a steady state concentration for level C.

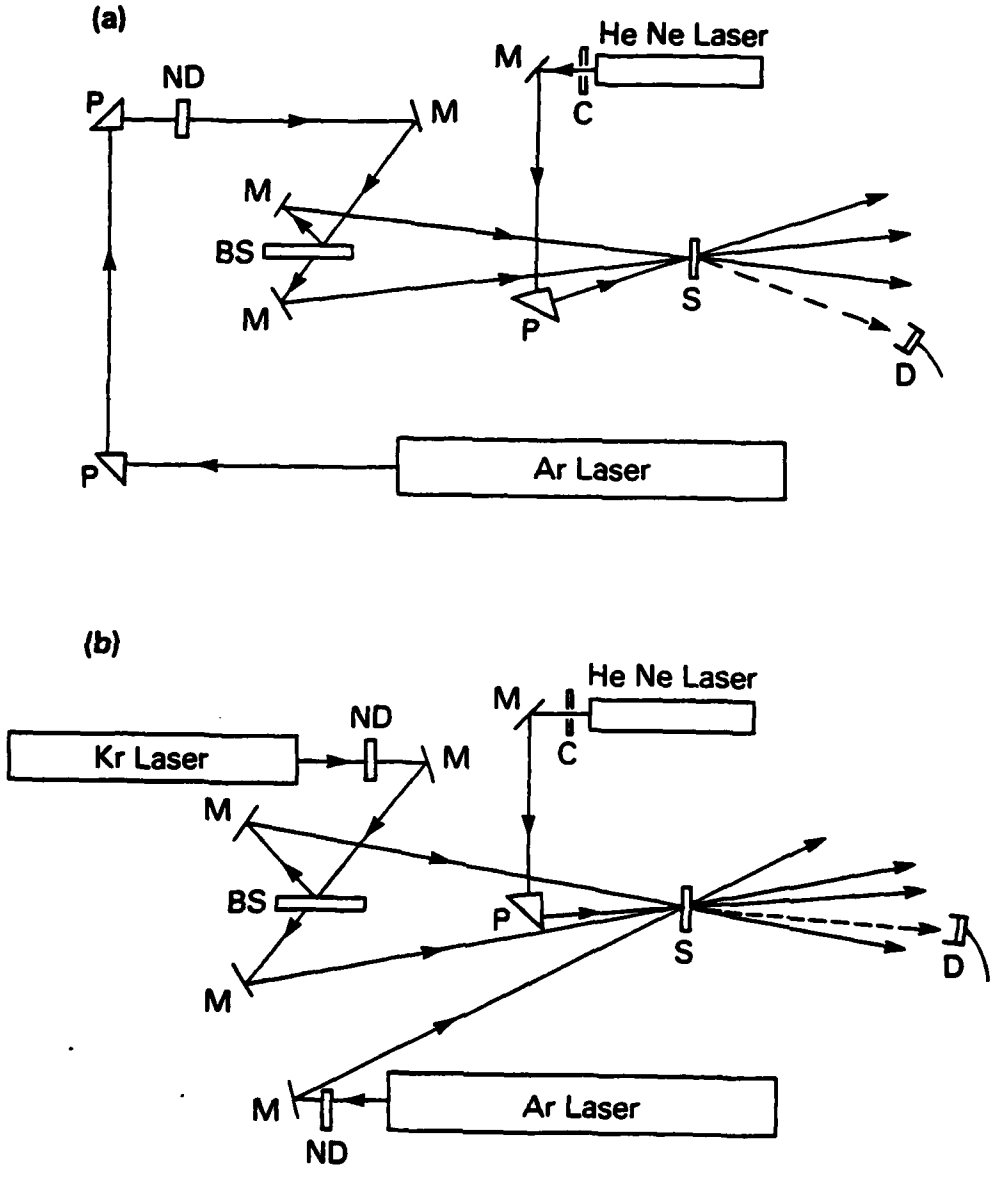

Figure 3. Experimental set up for a) one step and b) two step photochemical processes. In the figure P=prism, ND=neutral density filter, M=mirror, BS=beam splitter, C=chopper, S=hologram sample and D=detector.

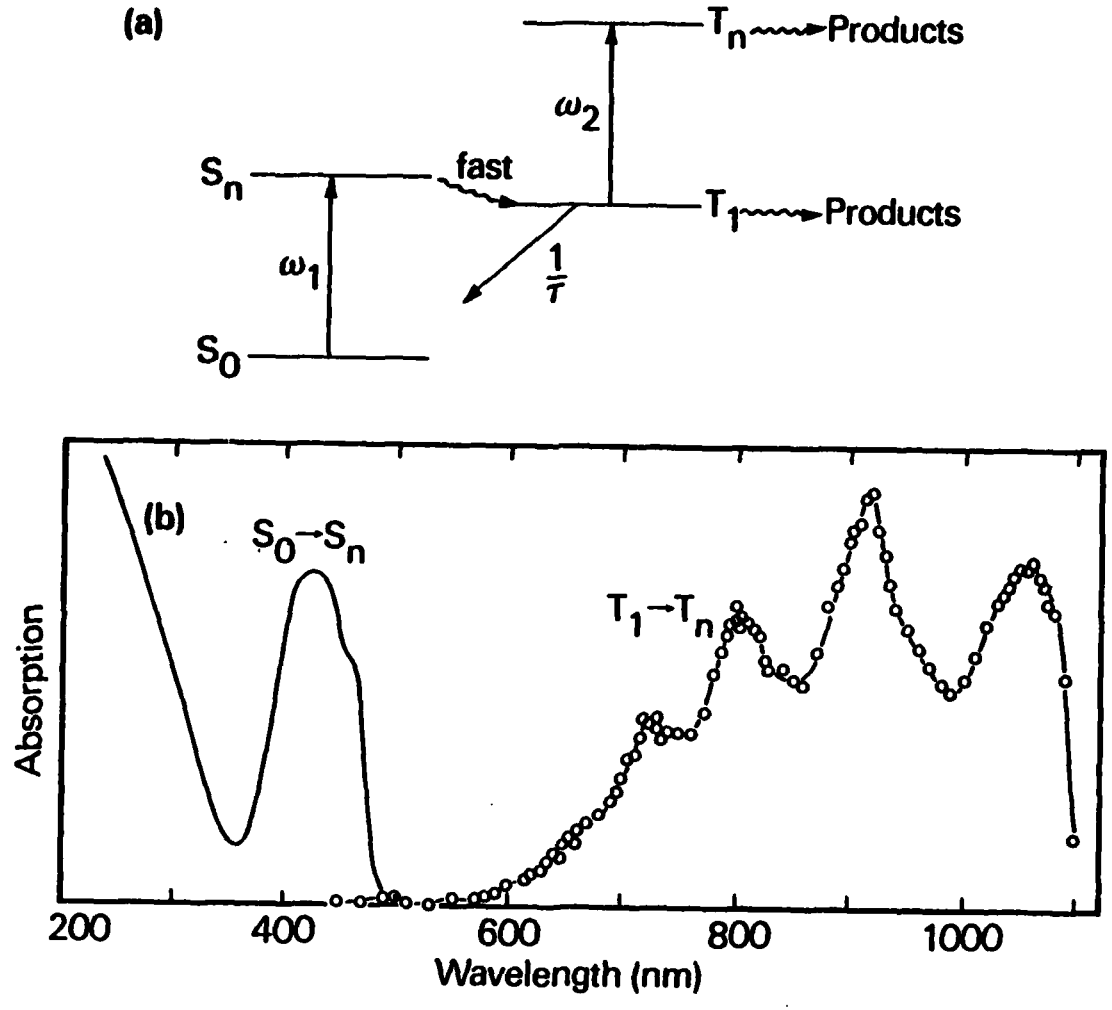

Figure 4. a) The energy level scheme for the one and two photon photochemistry of biacetyl. b) The singlet-singlet and triplet-triplet absorption of biacetyl. The triplet-triplet absorption is from Ref. 13.

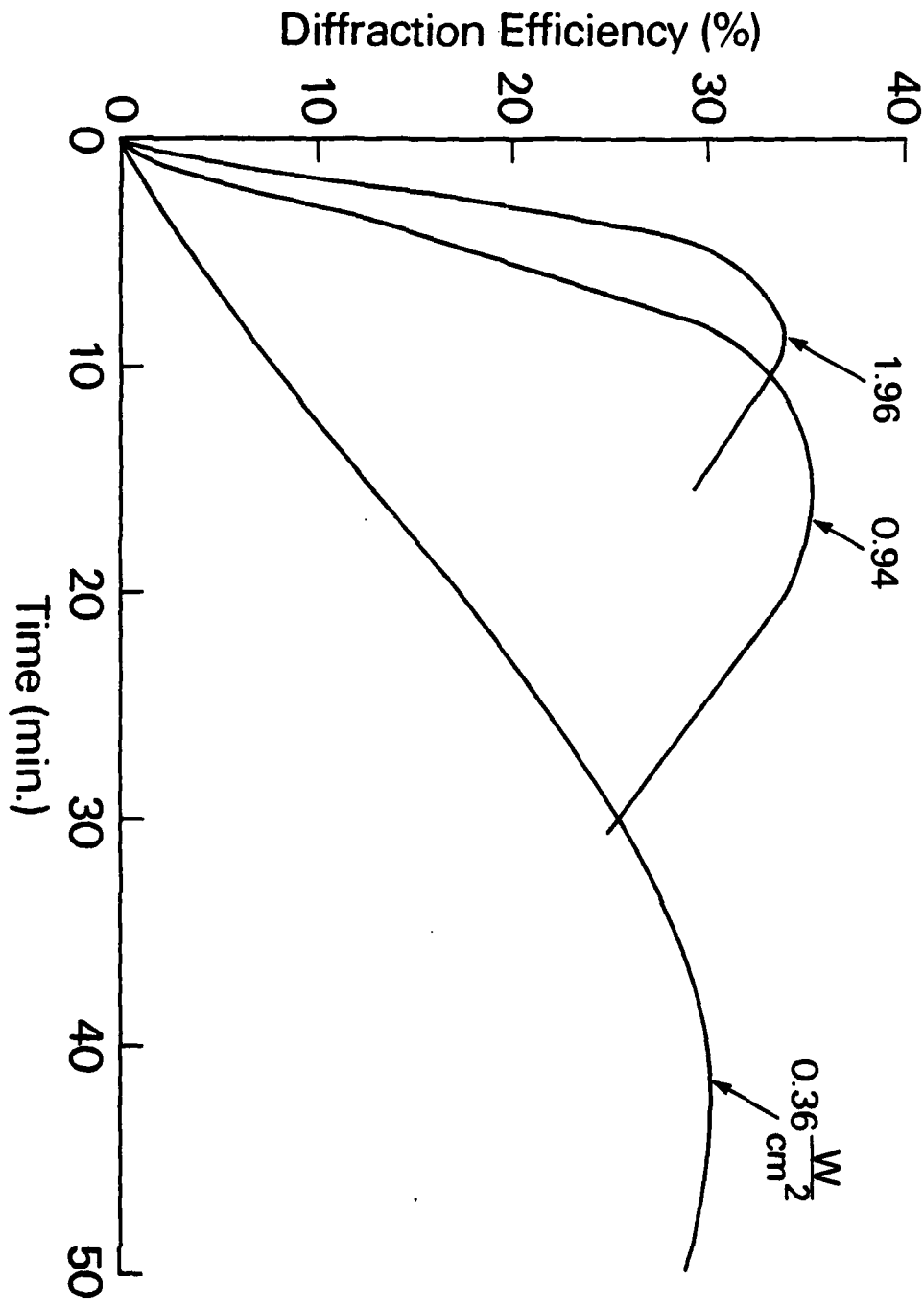

Figure 5. Hologram diffraction efficiency *versus* time for the one step photochemical reaction of biacetyl in polycyanoacrylate. Curves for three different power densities at 457.9 nm are shown.

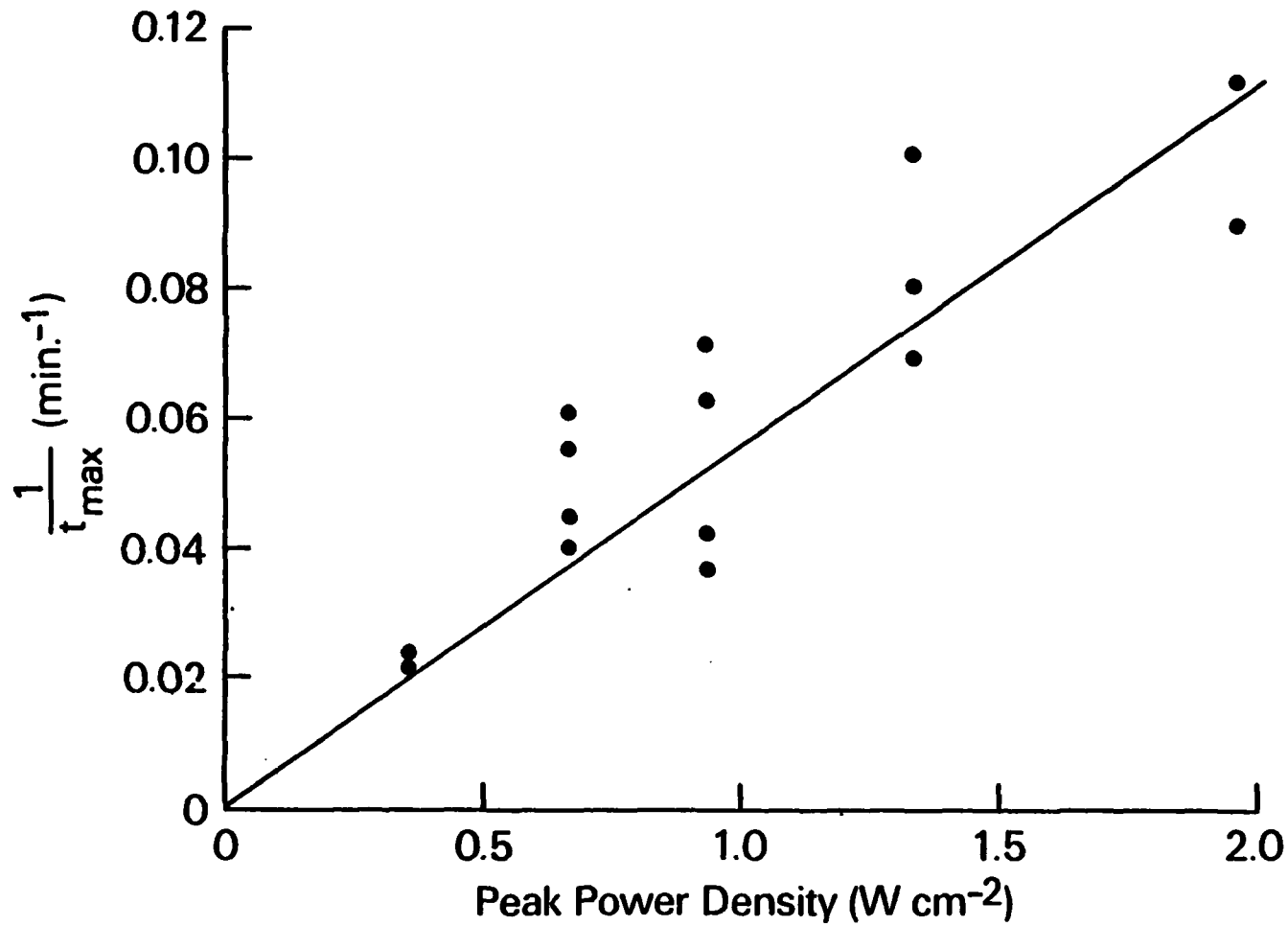

Figure 6. The inverse of the time for the hologram to reach its maximum efficiency *versus* the peak power density at 457.9 nm for the one step photochemical reaction. The solid line through the points is a least squares fit to the data including the origin.

Figure 7. a) The inverse of the time for the hologram to reach its maximum efficiency *versus* power density at 457.9 nm for the two step photochemical process. The infrared power density at 752.5 nm was held constant at 1.05 kW/cm^2. The solid line is a least squares fit to the data including the origin. b) The inverse of the time for the hologram to reach maximum efficiency *versus* peak power density at the 752.5 nm recording wavelength for the two step photochemical process. The 457.9 nm wavelength pumping light power density was held constant at 0.76 W/cm^2. The solid line is a least squares fit to the data including the origin, but ignoring the three highest power density points. These higher points are affected by softening of the polymer host.

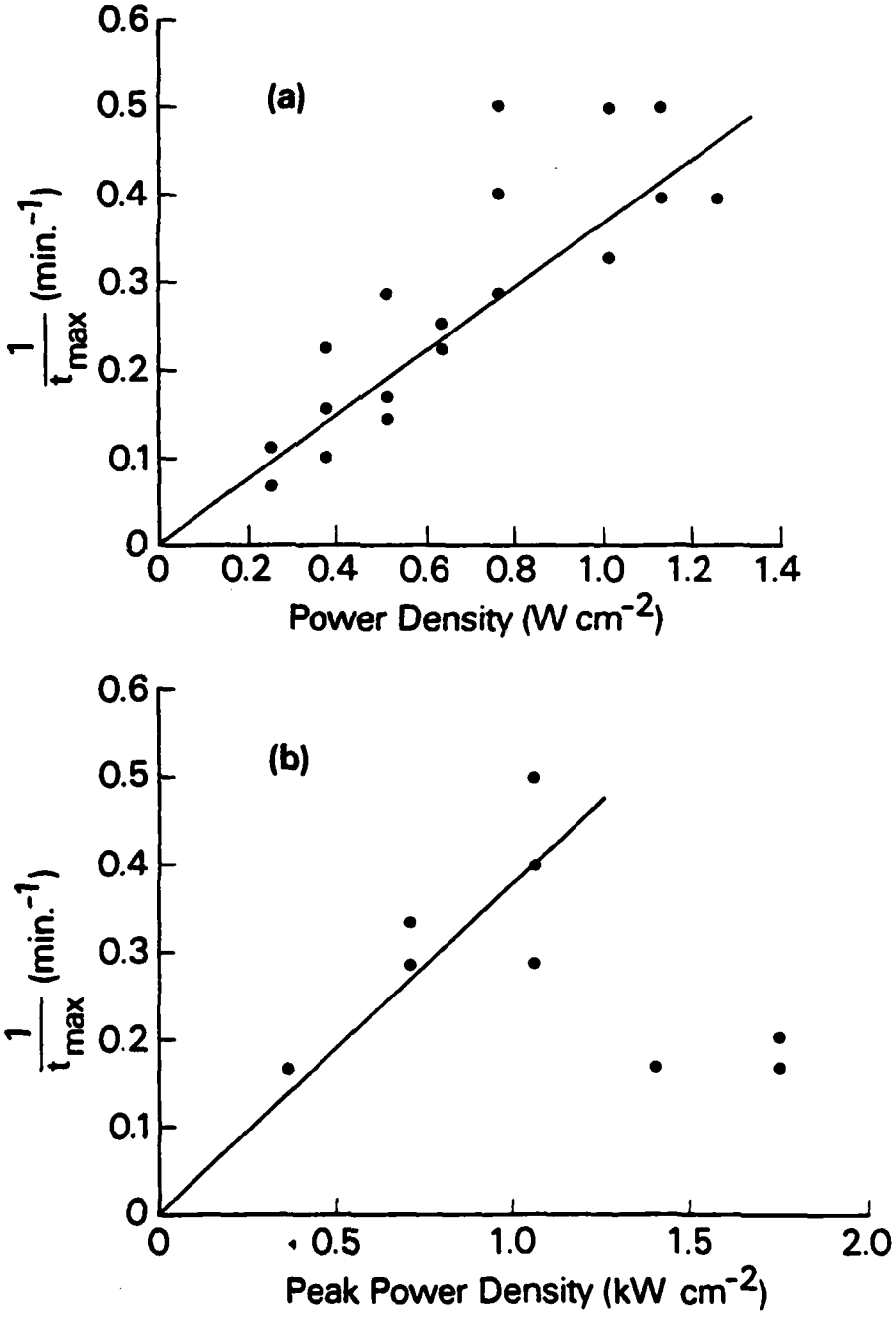

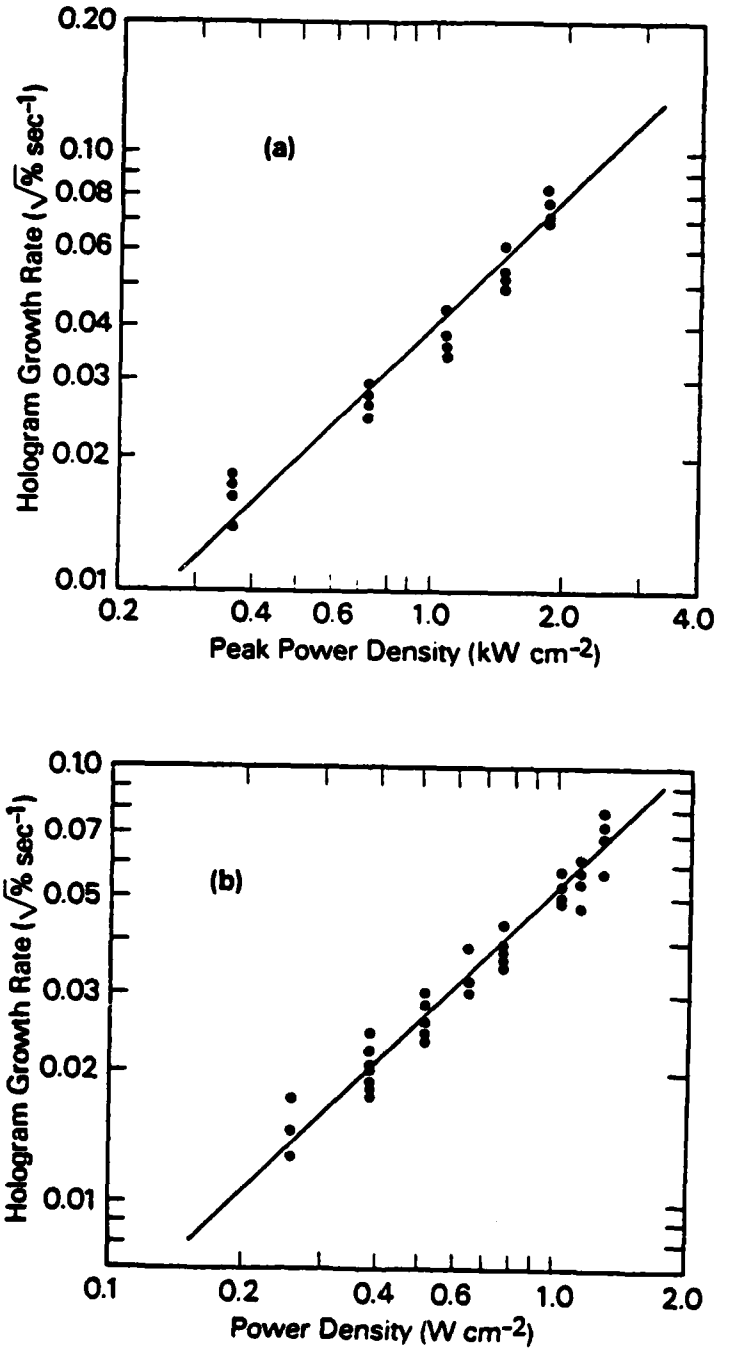

Figure 8. a) Hologram growth rate *versus* peak power density at 752.5 nm for the two step photochemical process. The solid line is calculated with a value of $|\delta n_A - \delta n_P|$ of 5.4×10^{-4}. b) Hologram growth rate *versus* peak power density at 457.9 nm for the two step photochemical process using the same value for $|\delta n_A - \delta n_P|$ as in a).

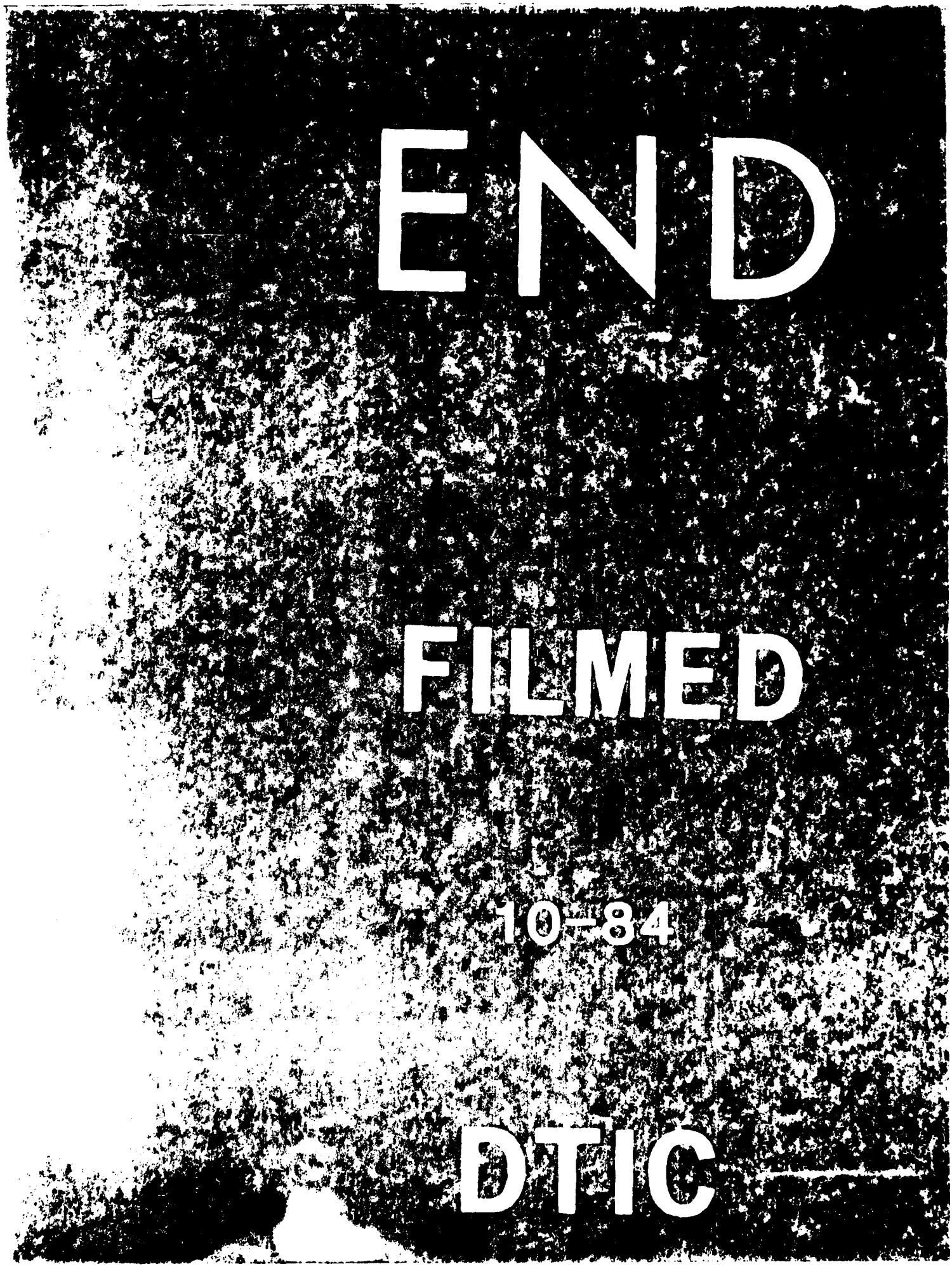
END
FILMED
10-84
DTIC